

Toward recognizing the vulnerable asymptomatic atheromatous plaque from B-mode ultrasound: the importance of the morphology of the plaque shoulder

S. Golemati¹, S. Lehareas¹, N. N. Tsiaparas², A. Gastounioti², A. Chatziioannou¹, K. S. Nikita², D. N. Perrea¹

¹Medical School, National & Kapodistrian University of Athens, Athens, Greece

²School of Electrical & Computer Engineering, National Technical University of Athens, Athens, Greece
sgolemati@med.uoa.gr, slehareas@gmail.com, ntsiapar@biosim.ntua.gr, gaimilia@biosim.ntua.gr, achatzi@med.uoa.gr, knikita@ece.ntua.gr, dperrea@med.uoa.gr

Abstract— Efficient management of the asymptomatic carotid disease remains a crucial challenge in clinical practice, because the ultrasonographically estimated degree of stenosis, which is currently used to determine treatment decisions, has been shown to be inadequate. In this study, texture (morphological) characteristics were investigated in a sample of asymptomatic male subjects, at the atheromatous plaque, the adjacent arterial wall and the plaque shoulder, i.e. the boundary between plaque and adjacent wall. A total of 25 arteries were interrogated, 11 with low (50-69%) and 14 with high (70-100%) degrees of stenosis. The two groups had similar ages. Texture characteristics were estimated from systolic and diastolic B-mode ultrasound images, and included four second-order statistical parameters (contrast, correlation, energy and homogeneity), each calculated at four different image directions (0° , 45° , 90° , 135°), yielding a total of 16 characteristics. Between high and low stenosis groups, 8 out of 16 characteristics were statistically different at the plaque shoulder at systole and 6 at diastole. No differences were observed between the two groups for any of the texture characteristics at the plaque nor at the adjacent wall. Differences in morphology along the arterial wall (wall - shoulder - plaque) were more pronounced in cases of high stenosis. The findings indicated that (a) the plaque shoulder is a particular area, requiring additional investigation so as to better understand the pathophysiology of atherosclerosis, (b) the phase of the cardiac cycle (systole or diastole) is important in texture analysis, and (c) the variability of morphology along the arterial wall, which is indicative of areas of tissue discontinuities, and therefore more vulnerable to rupture, can be characterized quantitatively with texture indices, toward an improved assessment of cardiovascular risk. It can be concluded that ultrasound-based texture indices may reveal novel markers for early detection and monitoring of subjects at high risk of cerebrovascular events, in the context of individualized, noninvasive and affordable diagnosis.

Keywords— Carotid; texture; plaque; shoulder; B-mode ultrasound

I. INTRODUCTION

The asymptomatic carotid atheromatous plaque is an arterial stenosis, which has not been associated with cerebrovascular events, such as strokes. Optimal management of the asymptomatic carotid disease is the subject of a growing controversy, in the context of which the benefits of revascularization, an invasive surgical procedure, are criticized

versus its drawbacks [1]. The alternative therapeutic strategy includes best medical (drug) treatment. To optimize clinical decision making, it is important to identify subgroups of subjects, for whom the benefits of a surgical procedure outweigh its risks. In other words, it is important to recognize subjects at high risk of suffering symptoms, i.e. subjects with a so-called vulnerable plaque.

Ultrasound-image-based indices seem to be promising in this respect. Ultrasound imaging is widely used in the diagnosis of carotid disease, due to its advantages, including non-invasiveness, real-time imaging, and low cost [2]. Furthermore, recent advances in computerized methods for ultrasound image analysis have allowed the extraction of features for describing tissue echogenicity/texture, motion/elasticity and morphology, thus providing additional information on plaque composition and stability [3]. The usefulness of such measures in enhancing the diagnostic procedure lies in their potential ability to discriminate between vulnerable and stable plaques as well as to characterize tissue modifications following specific therapeutic procedures.

Among ultrasound-image-based measures, texture analysis has gained attention as a determinant of plaque vulnerability. In carotid artery ultrasound images, texture quantifies the spatial distribution of gray levels in the imaged tissue, which, in turn, determines the pattern of allocation of echogenic (fibrous and calcified tissue) and anechoic (blood, lipids) materials.

A number of methods have been applied to estimate textural properties of B-mode ultrasound images of the carotid plaque. Among these, features derived from the gray tone spatial dependence matrices (GTSDM) [4], also called second-order statistical features, have been shown promising in the investigation of various arterial phenotypes. In combination with other texture features, GTSDM indices were able to characterize carotid plaques as symptomatic or asymptomatic [5]. GTSDM features have also been associated with ipsilateral neurological symptoms, including stroke and amaurosis fugax [6]. A recent important application of these

The project was funded in part by the Operational Program "Competitiveness and Entrepreneurship" and Regional Operational Programmes of the National Strategic Reference Framework (NSRF) 2007-2013. "SYNERGASIA": "Collaborative projects of small and medium scale". It was also partly funded by the John S. Latsis Public Benefit Foundation. The work of A. Gastounioti was also supported in part by a scholarship from the

particular texture features included their ability to predict high-risk asymptomatic plaques [7]. In addition to this, Niu et al have shown that GTSDM-based texture analysis can be used to identify optimal microbubble concentration in ultrasonic particle image velocimetry [8].

Thanks to their localized nature, texture features are able to quantify discrepancies between different tissue areas along the arterial wall. Accordingly, in this study, we sought to investigate the ability of GTSDM features to characterize tissue ultrasonic appearance of different parts of the diseased arterial wall, namely the wall proximal to the plaque, the plaque shoulder, i.e. the boundary between plaque and wall, and the plaque itself, in a sample of asymptomatic male subjects with various stenosis degrees.

II. MATERIALS & METHODS

A. Acquisition of Ultrasound Image Data

The investigated group included 25 arterial segments of elderly male patients with asymptomatic atherosclerotic carotid artery disease. Of these, 11 had low stenosis degrees (50-69%) and 14 had high stenosis degrees (70-100%). There was no statistical difference in the ages of the two groups (Wilcoxon rank sum test, p-value<0.05).

A Philips iU22 ultrasound scanner equipped with a 50-mm, 12-MHz linear-array transducer was used to acquire sequences of B-mode ultrasound images of the carotid arteries. Recordings were performed during breath holding, with the subjects in the supine position. Carotid arteries were scanned in the longitudinal direction using pre-defined settings (dynamic range, 65 dB; 2D gray map, linear; persistence, low; time gain compensation, neutral). Three sequences were recorded for each subject; one at the plaque site, one at the adjacent non-atherosclerotic wall, where the intima-media complex (IM) was clearly visible, and one at the so called plaque shoulder. The sequences were recorded at a rate of approximately 25 frames/s for 3–5 consecutive cardiac cycles and were stored for subsequent offline analysis. From each recording, one image corresponding to end-systole and one corresponding to end-diastole were isolated for manual outline and texture analysis.

The boundaries of atherosclerotic plaque, IM and plaque shoulder, in the corresponding images, were manually indicated by an expert physician. Fig. 1 shows examples of the recorded B-mode ultrasound images with the three different tissue types outlined.

B. Texture Analysis Using GTSDM-Derived Features

Estimation of GTSDM-derived features relies on the procedures introduced by Haralick et al [4], based on the assumption that the texture information in an image represents the overall or ‘average’ spatial relationship which the gray tones in the image have to one another. Specifically, it is assumed that this texture-context information is adequately determined by the matrix of relative frequencies P_{ij} , with which two neighboring pixels separated by distance d occur in the image, one with gray tone i and the other with gray tone j . Such matrices of gray tone spatial dependence frequencies are

a function of the distance between the neighboring pixels, as well as a function of the angular relationship between them ($P_{ij}(d, \theta)$). Typically, four different values of angular relationship are considered, namely 0° , 45° , 90° , and 135° (Fig. 2).

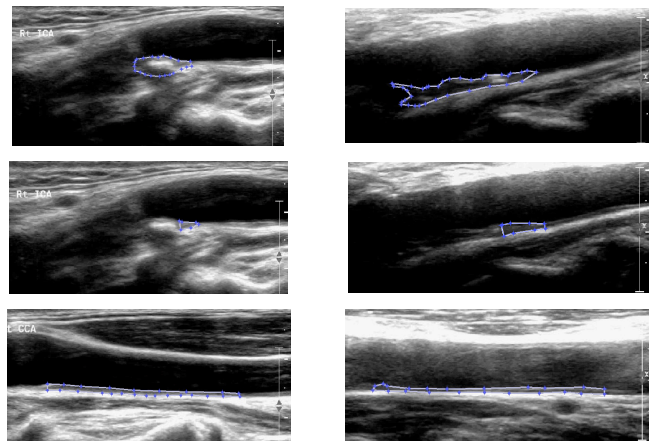


Fig. 1. B-mode ultrasound images of plaque (top row), plaque shoulder (middle row), and IM (bottom row), in a subject with low stenosis degree (left column) and one with high stenosis degree (right column). The investigated image areas were outlined by a physician. The images correspond to end-systole.

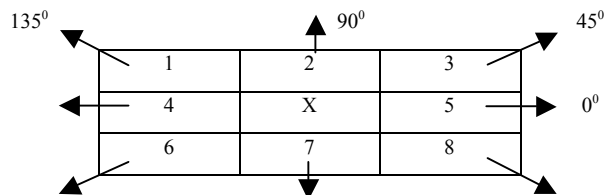


Fig. 2. Illustration of angular relationships between pixels 1-8, neighboring pixel X.

From these matrices, four texture features were extracted, namely contrast, also referred to as ‘variance’ in [4], correlation, energy, also referred to as ‘angular second moment’ in [4], and homogeneity, also referred to as ‘inverse difference moment’ in [4]. The equations for these texture features are given below:

$$Contrast = \sum_{i,j} |i - j|^2 P_{ij} \quad (1)$$

$$Correlation = \sum_{i,j} \frac{(i - \mu_i)(j - \mu_j) P_{ij}}{\sigma_i \sigma_j} \quad (2)$$

$$Energy = \sum_{i,j} P_{ij}^2 \quad (3)$$

$$Homogeneity = \sum_{i,j} \frac{P_{ij}}{1 + |i - j|} \quad (4)$$

where μ_i , μ_j , and σ_i , σ_j are the means and standard deviations, respectively, of the distributions associated with P_{ij} .

In this work, we used a distance value of 1 pixel ($d=1$) and calculated the four previously described texture features in each of the four different directions (0° , 45° , 90° , 135°); thus, we interrogated a total of 16 texture features for each image area. Texture features were estimated for systolic and diastolic images.

C. Statistical Analysis

Differences between features of low and high stenosis cases, as well as between different tissue areas (plaque, shoulder, IM), were quantified using the Wilcoxon rank-sum test. A p-value of 0.05 was considered significant.

Texture and statistical analyses were performed using Matlab software (MathWorks, Natick, Massachusetts, USA).

III. RESULTS

Fig. 3 shows examples of GTSDM. As we can see, increased values are present along the diagonal of the matrices, corresponding to relatively large values of pixel co-occurrences. These co-occurrences are somewhat more pronounced in the horizontal direction (0°), compared to the vertical (90°), which is representative of the horizontal allocation of the wall tissue material.

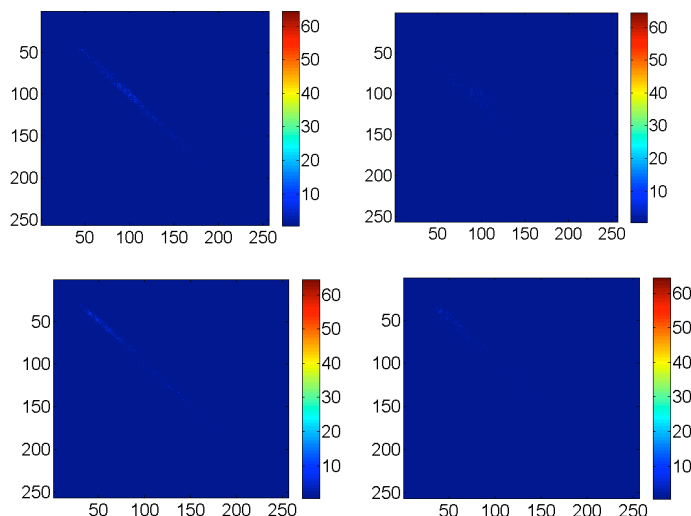


Fig. 3. GTSDM for wall (top row) and plaque (bottom row), for 0° (left column) and 90° (right column).

Differences between high and low stenosis groups were found for the plaque shoulder only. No differences were observed between the two groups for any of the texture characteristics neither at the plaque nor at the adjacent wall. More specifically, 8 out of the 16 interrogated texture features were statistically different at the plaque shoulder at systole and 6 at diastole (Table I). As we can see in Table I, the contrast was significantly higher, approximately double, in low stenosis cases, for both cardiac cycle phases and for all directions. Correlation was significantly lower in low stenosis cases, for both phases, for 0° and 45° . At systole, correlation

was significantly lower in low stenosis cases, also for 90° and 135° .

Table II shows the texture features that were significantly different between different wall areas in the low and high stenosis cases. As we can see, slightly more features (41 out of 48) were found different in high stenosis subjects, compared to low stenosis ones (35 out of 48).

TABLE II. TEXTURE FEATURES SIGNIFICANTLY DIFFERENT BETWEEN DIFFERENT TISSUE AREAS IN LOW AND HIGH STENOSIS CASES.

Plaque vs. shoulder	Wall vs. shoulder	Wall vs. plaque
<i>High stenosis (41 features)</i>		
Contrast ($0^\circ, 45^\circ, 90^\circ, 135^\circ$)	Contrast (0°)	Contrast ($45^\circ, 90^\circ, 135^\circ$)
Correlation ($0^\circ, 45^\circ, 90^\circ, 135^\circ$)	Correlation ($0^\circ, 45^\circ, 90^\circ$)	Correlation ($45^\circ, 90^\circ, 135^\circ$)
Energy ($0^\circ, 45^\circ, 90^\circ, 135^\circ$)	Energy ($0^\circ, 45^\circ, 90^\circ, 135^\circ$)	Energy ($0^\circ, 45^\circ, 90^\circ, 135^\circ$)
Homogeneity ($0^\circ, 45^\circ, 90^\circ, 135^\circ$)	Homogeneity ($0^\circ, 45^\circ, 90^\circ, 135^\circ$)	Homogeneity ($0^\circ, 90^\circ, 135^\circ$)
<i>Low stenosis (35 features)</i>		
Contrast ($0^\circ, 45^\circ, 90^\circ, 135^\circ$)	Contrast ($0^\circ, 45^\circ, 90^\circ, 135^\circ$)	Contrast ($45^\circ, 90^\circ, 135^\circ$)
Correlation ($0^\circ, 45^\circ, 90^\circ, 135^\circ$)	Correlation (0°)	Correlation ($45^\circ, 90^\circ, 135^\circ$)
	Energy ($0^\circ, 45^\circ, 90^\circ, 135^\circ$)	Energy ($0^\circ, 45^\circ, 90^\circ, 135^\circ$)
	Homogeneity ($0^\circ, 45^\circ, 90^\circ, 135^\circ$)	Homogeneity ($0^\circ, 45^\circ, 90^\circ, 135^\circ$)

IV. DISCUSSION

In this paper, texture features of carotid atheromatous plaque, plaque shoulder and adjacent nonatherosclerotic IM tissue were estimated from ultrasound images, in an attempt to quantify the allocation and structure of different tissue areas along the arterial wall of male asymptomatic subjects with various stenosis degrees.

Statistical analysis revealed significant differences in plaque shoulder characteristics between low and high stenosis groups; no differences were found neither for the plaque itself nor for the adjacent wall. This indicates the importance of the plaque shoulder region, which has been shown to be implicated in complex phenomena associated with diseases related to the cardiovascular system [9]. It is suggested that the properties of this arterial wall area be more intensely investigated in the context of the study of arterial disease.

GTSDM-based texture allows the extraction of valuable information about tissue structure and morphology along the arterial wall. In this case, it was shown that wall material is generally allocated in a horizontal direction. This type of allocation is more pronounced in the intima-media wall adjacent to the plaque, and is somewhat less obvious at the plaque area; the plaque shoulder is the most inhomogeneous

region. A similar observation was reported in [10], using a different texture analysis approach, namely a multiresolution method.

Systolic images produced slightly more features significantly different between high and low stenosis cases (8 vs. 6, Table I). This finding is in agreement with previous studies, in which multiresolution and multiscale texture features in systolic images yielded somewhat better classification performances of symptomatic and asymptomatic cases [10], [11].

Differences in morphology along the arterial wall (wall - shoulder - plaque, in the upstream direction) were more pronounced in cases of high stenosis, suggesting that texture variability may be associated to high-risk, vulnerable plaques, which are considered to be represented by high stenoses. These differences in texture features may be related to the strains experienced by the tissue under the effect of cardiovascular forces [12].

In conclusion, our findings indicated that (a) the plaque shoulder is a particular area, requiring additional investigation so as to better understand the pathophysiology of atherosclerosis, (b) the phase of the cardiac cycle (systole or diastole) is important in texture analysis, and (c) the variability of morphology along the arterial wall, which is indicative of areas of tissue discontinuities, and therefore more vulnerable to rupture, can be characterized quantitatively with texture indices, toward an improved assessment of cardiovascular risk. Thus, ultrasound-based texture indices may reveal novel markers for early detection and monitoring of subjects at high risk of cerebrovascular events, in the context of individualized, noninvasive and affordable diagnosis.

REFERENCES

[1] S. Venkatachalan, "Asymptomatic carotid stenosis: immediate revascularization or watchful waiting?" *Curr Cardiol Rep*, vol. 16, no. 1, pp. 440, Jan. 2014.

[2] J. Eydin, B. Geier, and D. Staub, "Current strategies and possible perspectives of ultrasonic risk stratification of ischemic stroke in internal carotid artery disease," *Ultraschall Med*, vol. 32, no. 3, pp. 267-273, Jun. 2011.

[3] S. Golemati, A. Gastouniotti, and K.S. Nikita, "Toward novel noninvasive and low-cost markers for predicting strokes in asymptomatic carotid atherosclerosis: the role of ultrasound image analysis," *IEEE Trans. Biomed. Eng.*, vol. 60, no. 3, pp. 652-658, Mar. 2013.

[4] R. Haralick, K. Shanmugam, and I. Dinstein, "Textural features for image classification," *IEEE Trans Syst Man Cybern*, vol. SMC-3, no. 6, pp. 610-621, Nov. 1973.

[5] C. I. Christodoulou, C. S. Pattichis, M. Pantziaris, and A. Nicolaides, "Texture-based classification of atherosclerotic carotid plaques," *IEEE Trans Med Imag*, vol. 22, no. 7, pp. 902-912, Jul. 2003.

[6] S. K. Kakkos, A. N. Nicolaides, E. Kyriacou, et al. "Computerized texture analysis of carotid plaque ultrasonic images can identify unstable plaques associated with ipsilateral neurological symptoms," *Angiology*, vol. 62, no. 4, pp. 317-328, May 2011.

[7] E. C. Kyriacou, S. Petroudi, C. S. Pattichis, et al. "Prediction of high-risk asymptomatic carotid plaques based on ultrasonic image features," *IEEE Trans Inf Technol Biomed*, vol. 16, no. 5, pp. 966-973, Sep. 2012.

[8] L. Niu, M. Qian, L. Yan, et al. "Real-time texture analysis for identifying optimum microbubble concentration in 2-D ultrasonic particle image velocimetry," *Ultrasound Med Biol*, vol. 37, no. 8, pp. 1280-1291, Aug. 2011.

[9] F. J. Olson, S. Strömberg, O. Hjelmgren, et al, "Increased vascularization of shoulder regions of carotid atherosclerotic plaques from patients with diabetes," *J Vasc Surg*, vol. 54, no. 5, pp. 1324-1331, Nov. 2011.

[10] N. N. Tsiaparas, S. Golemati, I. Andreadis, J. S. Stoitsis, I. Valavanis, and K. S. Nikita, "Comparison of multiresolution features for texture classification of carotid atherosclerosis from b-mode ultrasound," *IEEE Trans Inf Technol Biomed*, vol. 15, no. 1, pp. 130-137, Jan. 2011.

[11] N. N. Tsiaparas, S. Golemati, I. Andreadis, J. S. Stoitsis, I. Valavanis, and K. S. Nikita, "Assessment of carotid atherosclerosis from b-mode ultrasound images using directional multiscale texture features," *Meas Sci Technol*, vol. 23, 10 pp, 2012.

[12] A. Gastouniotti, S. Golemati, and K. S. Nikita, "Computerized analysis of ultrasound images: potential associations between texture and motion properties of the diseased arterial wall," *Proc IEEE Int Ultrasonics Symp*, pp. 691-694, Oct. 2012.

TABLE I. AVERAGE±STANDARD DEVIATION VALUES OF TEXTURE FEATURES FOR HIGH (HS) AND LOW (LS) STENOSIS CASES AT PLAQUE SHOULDER FOR DIASTOLE AND SYSTOLE.

	Texture feature	Diastole		Systole	
		HS (n=14)	LS (n=11)	HS (n=14)	LS (n=11)
1	Contrast (0°)	384.04±303.30	829.72±658.73	399.96±289.64	994.63±841.84
2	Contrast (45°)	986.46±520.94	1975.38±1416.30	1023.69±525.71	2309.90±2226.81
3	Contrast (90°)	930.08±474.16	1659.06±1131.06	934.73±443.30	1910.03±1587.77
4	Contrast (135°)	1171.31±646.58	1980.88±1258.11	1166.20±580.99	2267.309±1708.22
5	Correlation (0°)	0.950±0.032	0.905±0.053	0.950±0.031	0.885±0.051
6	Correlation (45°)	0.863±0.069	0.771±0.123	0.868±0.060	0.740±0.119
7	Correlation (90°)	0.867±0.070	0.807±0.099	0.877±0.056	0.783±0.091
8	Correlation (135°)	0.836±0.086	0.764±0.115	0.848±0.069	0.736±0.103
9	Energy (0°)	0.136±0.060	0.169±0.058	0.148±0.077	0.187±0.054
10	Energy (45°)	0.114±0.064	0.132±0.052	0.124±0.078	0.149±0.056
11	Energy (90°)	0.120±0.062	0.149±0.060	0.132±0.076	0.167±0.056
12	Energy (135°)	0.113±0.060	0.138±0.055	0.123±0.075	0.155±0.057
13	Homogeneity (0°)	0.541±0.058	0.554±0.061	0.547±0.067	0.575±0.052
14	Homogeneity (45°)	0.423±0.081	0.428±0.086	0.430±0.096	0.456±0.075
15	Homogeneity (90°)	0.436±0.076	0.454±0.086	0.445±0.088	0.488±0.073
16	Homogeneity (135°)	0.418±0.075	0.435±0.090	0.426±0.090	0.465±0.073

Boldface indicates statistically significant differences (Wilcoxon ranksum test, p-value<0.05) compared to HS. n: number of interrogated cases.